

PARC ANALYSIS OF HSR NOZZLES

Nicholas J. Georgiadis
NASA Lewis Research Center
Cleveland, Ohio

518-07

PARC FNS ANALYSES:

1. **3D ANALYSIS OF PRATT & WHITNEY 2D MIXER-EJECTOR NOZZLE (Y. CHOI)**
2. **AXISYMMETRIC ANALYSIS OF NASA LANGLEY SINGLE FLOW PLUG NOZZLE (N. GEORGIADIS)**

Only recently has computational fluid dynamics (CFD) been relied upon to predict the flow details of advanced nozzle concepts. Computer hardware technology and flow solving techniques are advancing rapidly and CFD is now being used to analyze such complex flows. Validation studies are needed to assess the accuracy, reliability, and cost of such CFD analyses. At NASA Lewis, the PARC2D/3D full Navier-Stokes (FNS) codes are being applied to HSR-type nozzles. This report presents the results of two such PARC FNS analyses. The first is an analysis of the Pratt and Whitney 2D mixer-ejector nozzle, conducted by Dr. Yunho Choi (formerly of Sverdrup Technology-NASA Lewis Group). The second is an analysis of NASA-Langley's axisymmetric single flow plug nozzle, conducted by the author.

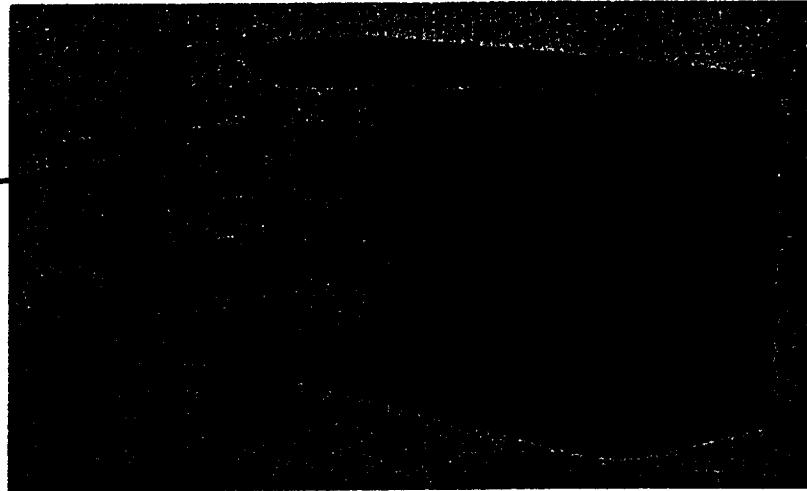
OVERVIEW OF PARC:

- **3D AND 2D/AXISYMMETRIC VERSIONS**
- **NAVIER-STOKES AND EULER MODES**
- **CENTRAL DIFFERENCING-BEAM AND WARMING ALGORITHM**
- **TURBULENCE MODELS:**
 - 1. THOMAS (STANDARD ALGEBRAIC MODEL)**
 - 2. BALDWIN-LOMAX**
 - 3. K-EPSILON**

The PARC2D/3D internal flow Navier-Stokes codes¹ are used to analyze a variety of propulsion flows. PARC solves the Reynolds-averaged Navier-Stokes equations in conservation law form with the Beam and Warming approximate factorization algorithm². Both algebraic and two-equation turbulence models are available in PARC to analyze turbulent flows. The algebraic turbulence models are the P.D. Thomas model³ and the Baldwin-Lomax model⁴. The two-equation models are the Chien low Reynolds number $k-\epsilon$ model⁵ (modified for compressibility by Nichols⁶ and added to the 2D/axisymmetric PARC code in 1990) and the Speziale low Reynolds number $k-\epsilon$ model⁷ (added to the 3D PARC code in 1991).

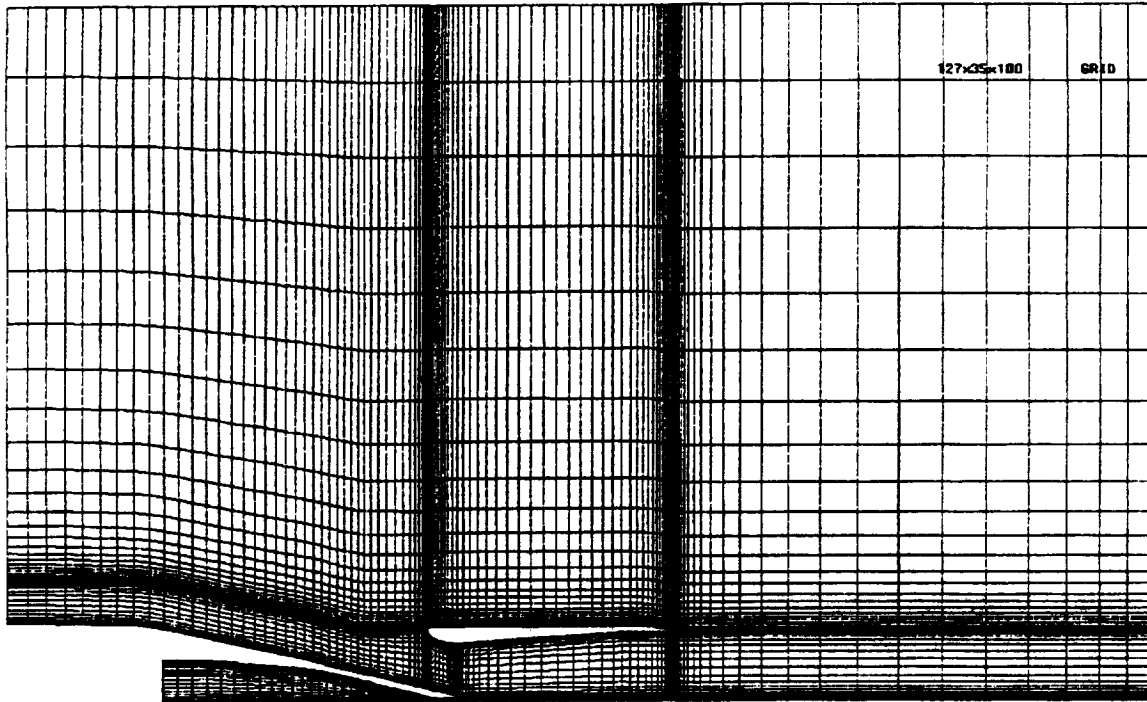
PRATT & WHITNEY 2D MIXER-EJECTOR NOZZLE GEOMETRY

CROSS SECTION
MODELLED



The first of the two PARC analyses discussed in this report was the 3D calculation of the flowfield of the Pratt and Whitney 2D mixer-ejector nozzle that was tested in the NASA Lewis (LeRC) 9' x 15' wind tunnel. A cut-away view of the nozzle geometry is shown in the figure. The configuration shown, with the short shroud enclosing the mixing region (as opposed to the intermediate length and long shrouds) is the one considered in the analysis described here. A parallel analysis of this nozzle was conducted by United Technologies Research Center (UTRC) using a Pratt and Whitney finite volume Navier-Stokes code, NASTAR. The two codes were used to calculate the nozzle flowfield for the case having the following operating conditions: Free stream pressure = 14.5 psia, free stream total temperature = 530° R, primary total temperature = 1960° R, and nozzle pressure ratio (NPR) = 4. The two codes' predictions of this flow case were compared to experimental data collected in the LeRC 9' x 15' wind tunnel tests.

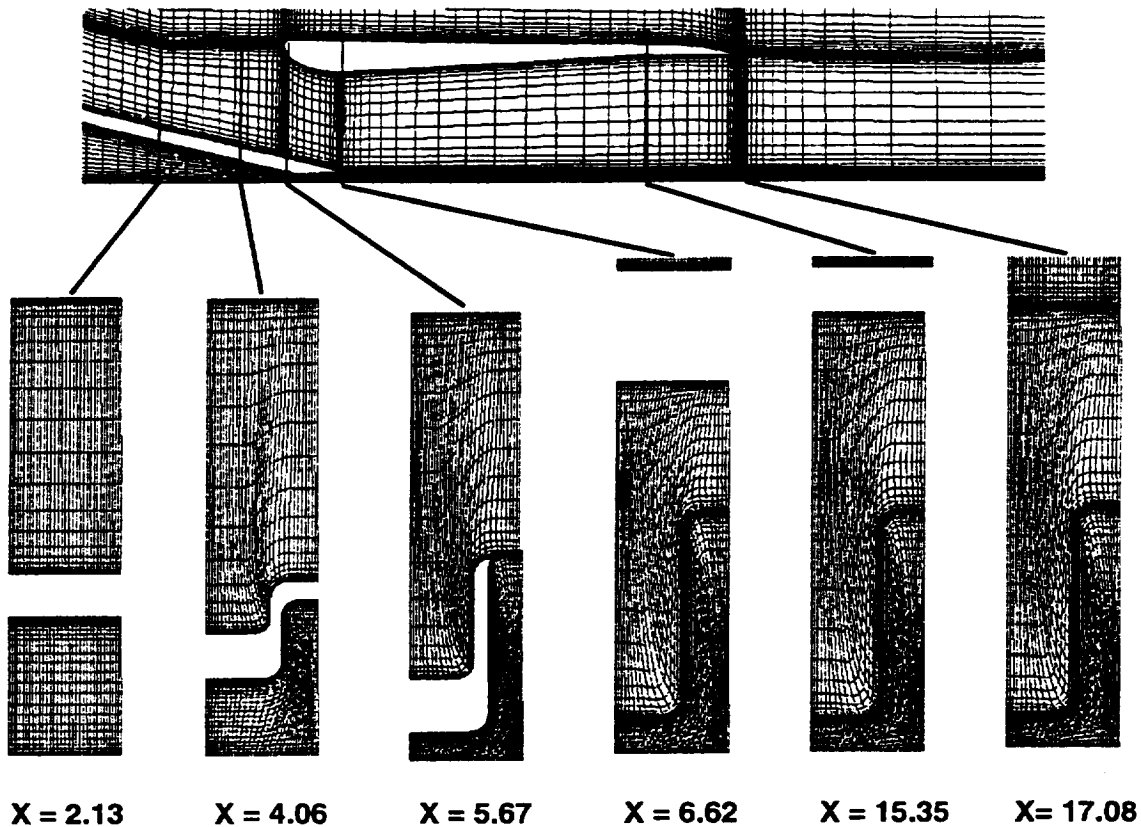
3D COMPUTATIONAL GRID FOR NOZZLE FLOWFIELD



Generation of the 3D computational grid required significant effort. Two grids were constructed for the Pratt and Whitney 2D mixer-ejector nozzle. The first was composed of three blocks (one each for the following regions: upstream of the nozzle, in the mixer, and downstream of the mixer) and had a total of 493,500 points. The second was a single block grid with 444,500 points. The grid shown in the figure is the single block grid; however, the multiblock grid looks nearly the same as that shown in this figure.

The two grids were initially constructed to compare the accuracy and efficiency of the PARC code in using single block and multiblock grids for the same flow case. After a series of iterations had been conducted for both cases, it was determined that the multiblock solution was having much difficulty converging at one of the block interfaces. The multiblock grid case was then stopped and the rest of this report will only discuss the single block case.

AXIAL CUTS THROUGH 3-D GRID

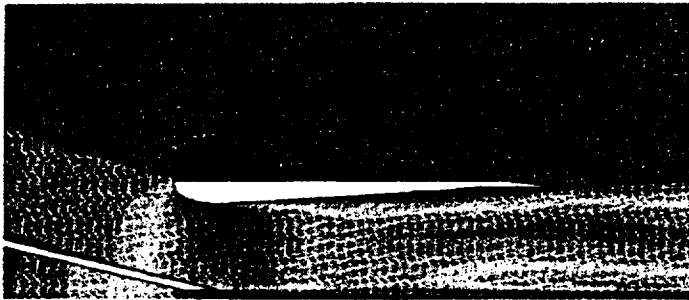


The figure shows six axial cuts through the single block grid in order to demonstrate the complexity of the grid. The first two sections ($X = 2.13$ and $X = 4.06$) are cut through the primary nozzle and ejector inlet. The third section ($X = 5.67$) is at the leading edge of the shroud. The fourth section ($X = 6.62$) is cut through the shroud at its maximum thickness position. The fifth section ($X = 15.35$) cuts through the shroud at approximately 85 percent chord. The sixth cut ($X = 17.08$) is just downstream of the shroud's trailing edge.

MACH NUMBER CONTOURS FOR P&W MIXER-EJECTOR NOZZLE



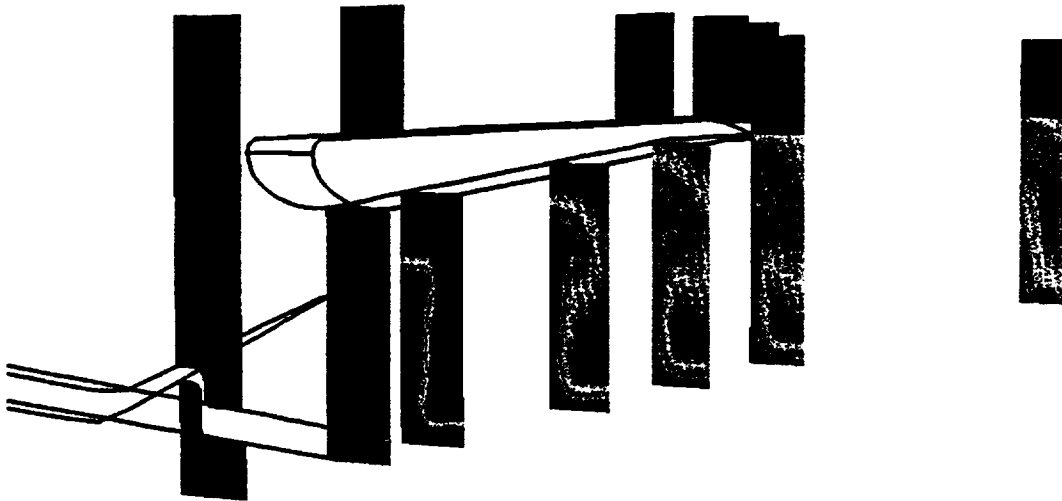
PEAK SIDE



VALLEY SIDE

Mach number contours in the planes of the peak side and valley side of the primary nozzle are shown in the figure. The primary flow chokes within the primary nozzle and expands to over Mach 2.0 downstream of the primary nozzle exit. The secondary flow entering the mixing region chokes near the maximum thickness location of the shroud. The peak side Mach number contour plot shows that two high energy flow streaks (one down the centerline and the second extending through the mixing region near the shroud) continue past the exit of the mixing region.

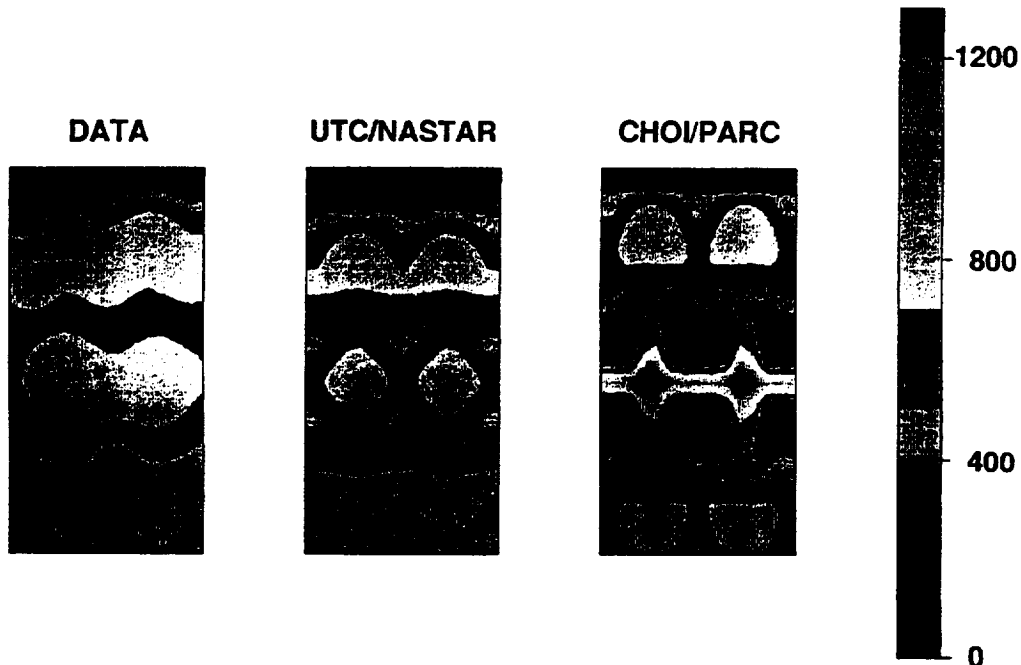
TOTAL TEMPERATURE CONTOURS FOR P&W MIXER-EJECTOR NOZZLE



The total temperature contours (shown at several cross sections beginning in the primary nozzle and extending past the shroud exit) also show the two hot streaks. At the mixing region exit plane, the total temperature at the centerline remains at the primary total temperature while the total temperature in the other hot streak decreases to about 65 percent of the primary total temperature.

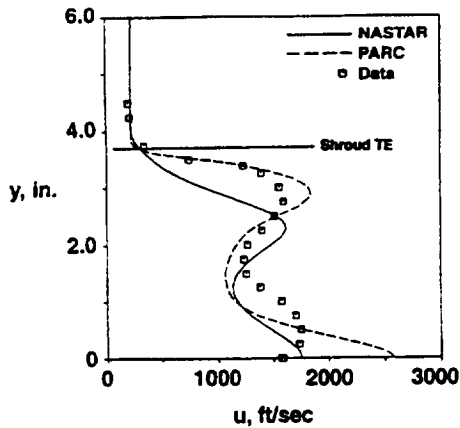
2nd GENERATION MIXER EJECTOR ANALYSIS

Exit Plane Total Temperature

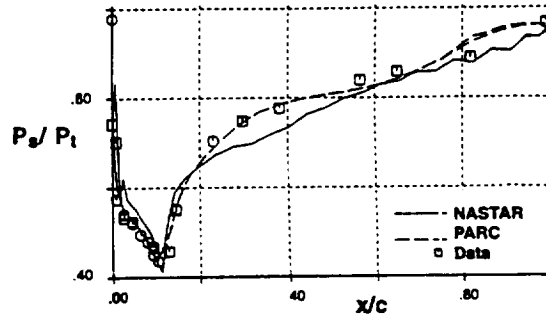


A comparison of experimental data obtained in the LeRC 9' x 15' tests to the PARC calculation and UTRC's NASTAR calculation of the total temperature field slightly downstream of the shroud exit plane is shown in the figure (taken from a Pratt and Whitney presentation). The two CFD solutions are each reflected about the planes of symmetry for comparison to the data. Both CFD solutions demonstrate less mixing than does the experimental data, with the PARC solution demonstrating less mixing than the NASTAR solution. The major differences between the codes used to obtain the two solutions are that PARC is a finite difference code and used the Thomas algebraic turbulence model while NASTAR is a finite volume code and used the $k-\epsilon$ turbulence model.

COMPARISON OF CFD RESULTS TO EXPERIMENTAL DATA



VELOCITIES AT EXIT PLANE



PRESSURES ALONG SHROUD

The comparison between experimental data and CFD calculations of velocity profiles at the shroud exit plane in the left side of the figure also shows that the PARC solution underpredicts the extent of mixing. The position of the two velocity peaks (one at the centerline and the other close to the shroud) correspond to the positions of the total temperature peaks shown in a previous figure. The comparison of static pressures along the shroud (shown in the right side of the figure) show that the PARC solution matches the experimental data well. The PARC solution predicted the pumping ratio (secondary flow rate divided by primary flow rate) to be 1.51. This also matches the experimental data (pumping ratio = 1.46) well.

LONG SHROUD CALCULATION

- SAME FLOW CONDITIONS AS FOR SHORT SHROUD
- NEW SHROUD LENGTH: (1.7 x SHORT SHROUD LENGTH)



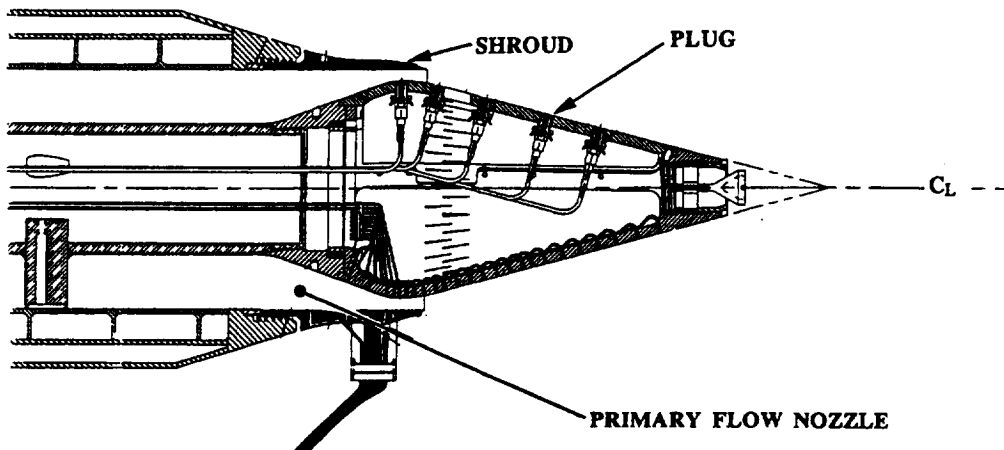
- MIXING ENHANCED (COMPARED TO SHORT SHROUD):
 - (1) ~20% LOWER MAXIMUM EXIT VELOCITY
 - (2) ~25% LOWER STAGNATION PRESSURE AND TEMPERATURE
- PUMPING UNCHANGED

After completion of the short shroud case, calculations were also made for a long shroud case. The figure shows a comparison between the cross sections of the short shroud and the long shroud (length = 1.7 x short shroud). The operating conditions of the nozzle and free stream were the same as for the short shroud case. The same size grid (444,500 points) was also used for the calculations.

The long shroud results indicated that mixing was enhanced relative to the short shroud solution. At the exit plane, the maximum velocity at the centerline decreased by 20 percent relative to the short shroud case and the maximum total pressures and temperatures decreased by about 25 percent. The secondary flow pumping was unchanged from the short shroud case.

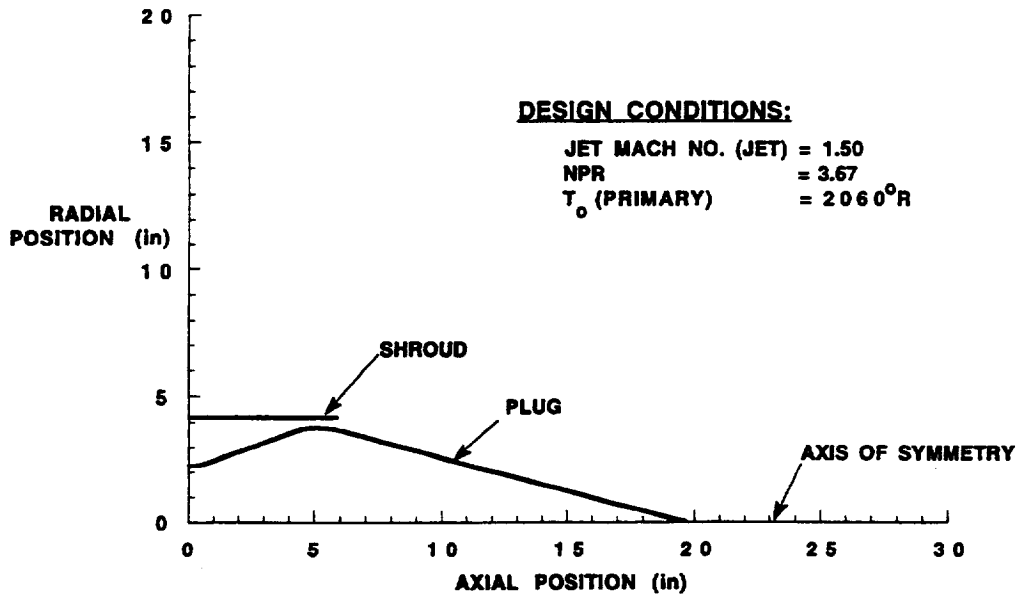
LANGLEY SINGLE FLOW PLUG NOZZLE

- VENTED AND NON-VENTED PLUGS
- 15° PLUG HALF ANGLE
- HEAVILY INSTRUMENTED TO MEASURE:
 1. PLUG SURFACE TEMPERATURES, PRESSURES, SHEAR STRESS
 2. JET PLUME QUANTITIES (INCLUDING LDV & FLOW VISUALIZATION)
 3. FLOWFIELD ACOUSTICS



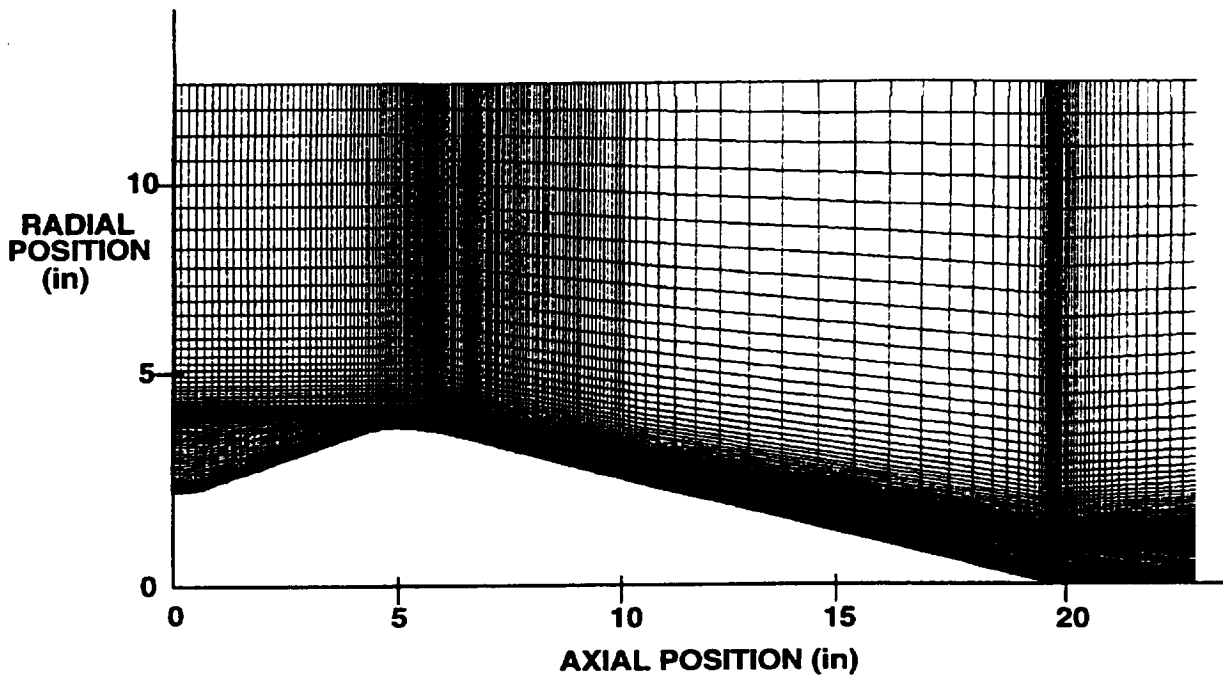
The second analysis is that of the NASA Langley single flow plug nozzle (conducted with the PARC2D/axisymmetric code). This nozzle will be tested in NASA Langley's Jet Noise Laboratory (JNL) and will provide an extensive set of data for CFD code validation. During these tests, Dr. Jack Seiner of NASA Langley⁸ intends to measure several quantities including temperatures, pressures, shear stress, and heat transfer along the plug; pressures, temperatures, velocity profiles, and Reynolds stresses (with LDV) in the plume; and acoustics in the flowfield. The plug will be removable to allow for installation of a ventilated plug (to control flow separation and shocks occurring between the plug surface and the free shear layer that forms between the primary flow and the surrounding air).

GEOMETRY FOR GRID GENERATION AND PARC2D CALCULATIONS



The geometry of the nozzle flow field modelled in the PARC calculations is shown in this figure. The axial and radial coordinate axes shown in this figure are the same for the rest of the plots in this report. A splitter plate (.020 inches thick) separates the primary flow from the ambient air and extends to $X = 5.8$ inches. The plug has a 15 degree half angle that extends to $X = 19.6$ inches. The nozzle area ratio and NPR are set to provide a Mach number of 1.50 at the nozzle exit plane. The total temperature of the primary flow is 2060° R. In the JNL tests, the primary nozzle flow will exit into quiescent air. For the PARC calculations, the freestream Mach number was set to Mach 0.3 because PARC (like many FNS codes) has difficulty in converging very low Mach number (incompressible) flows.

GRID FOR PARC2D CALCULATIONS OF LANGLEY SINGLE FLOW PLUG NOZZLE



Several grids (having different numbers of grid points but representing the same physical space) were constructed with the INGRID code. The figure shows one of the computational grids in the vicinity of the nozzle. The physical size of all the grids was 120 inches in the axial direction (in order to model the jet mixing with the ambient air far downstream of the plug tip) by 12 inches in the radial direction. In the following comparisons of flowfield solutions, three grids are referred to as coarse, medium, and fine. The sizes of these grids were 237 x 145, 315 x 145, and 415 x 129, respectively.

TURBULENCE MODELS IN PARC:

A. ALGEBRAIC MODELS:

1. P.D. THOMAS

- STANDARD ALGEBRAIC MODEL IN PARC
- OPTIMIZED FOR FREE SHEAR LAYERS

2. BALDWIN-LOMAX

- OPTIMIZED FOR ATTACHED WALL BOUNDED FLOWS

B. 2-EQUATION MODELS (k- ϵ):

1. CHIEN (Low Re) - PARC2D/AXISYMMETRIC

2. SPEZIALE (Low Re) - PARC3D

The figure shows the turbulence models that are currently available in the PARC code. The standard algebraic turbulence model in PARC is based upon the work of P.D. Thomas. This model calculates turbulent viscosity near surfaces (wall-bounded part of model) and in regions where flows are mixing (free shear layer part of model) but was optimized for the latter. The Baldwin-Lomax model only calculates turbulent viscosity in wall-bounded regions. These two algebraic models may also be run in conjunction (Baldwin-Lomax for wall-bounded regions and Thomas model only in free shear layer regions) to provide a third algebraic model.

These algebraic models are all simple mixing length models that use an empirically determined turbulent mixing length distribution to calculate turbulent viscosity. These models often model complex flows inadequately because their mixing length distributions are not applicable to all flows. Two-equation models (such as k- ϵ) avoid this single mixing length limitation by solving additional transport equations to calculate turbulent viscosity but are substantially more computationally expensive than the algebraic models. As mentioned previously, k- ϵ models have been added recently to the PARC code (Chien low Reynolds number model in the 2D/axisymmetric code and the Speziale low Reynolds number model in the 3D code). The three algebraic turbulence models (Thomas, Baldwin-Lomax/Thomas combination, and Baldwin-Lomax) and the Chien k- ϵ turbulence model were used for the initial PARC calculations.

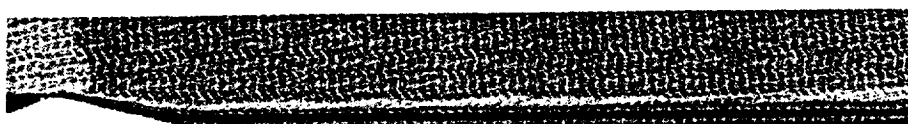
MACH NUMBER CONTOURS ALONG PLUG AND IN JET PLUME



Thomas



Baldwin-Lomax
/Thomas



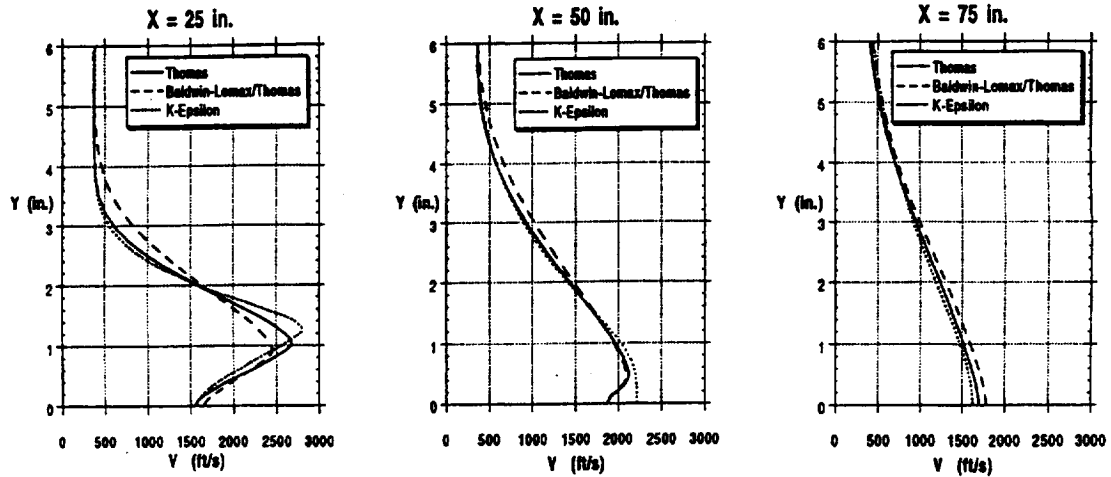
Baldwin-Lomax



K-Epsilon

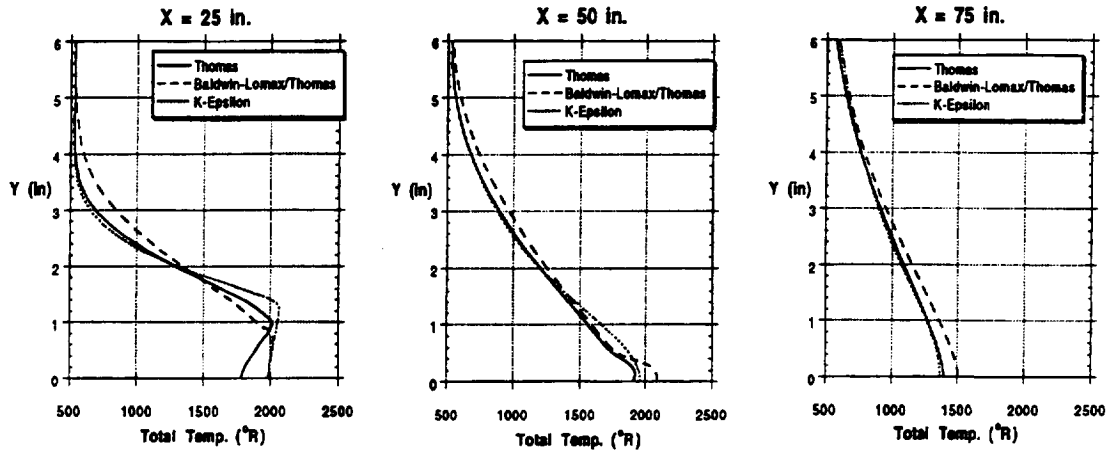
The figure shows Mach number contours for the flow region extending from the entrance of the nozzle and freestream out to the plume at approximately $X = 80$ inches for the four turbulence models that were initially considered using the coarse grid. The plume of the $k-\epsilon$ solution (bottom contour plot) decays most rapidly. The Baldwin-Lomax plot (second from the bottom) shows that there is essentially no dissipation of the flow after the plug tip. This occurs because the Baldwin-Lomax model calculates turbulent viscosity only in wall bounded regions. After the plug tip ($X = 19.6$ inches), there is no solid surface, so no turbulent viscosity is being calculated there. The combination Baldwin-Lomax/Thomas solution (contour plot just above Baldwin-Lomax) was obtained by calculating turbulent viscosity in the wall bounded regions of the nozzle with Baldwin-Lomax and in the jet plume with the free shear layer model part of the Thomas model. Because Baldwin-Lomax (alone, with no free shear layer model) has the limitation of not being able to calculate turbulent viscosity in the plume, it was only used to obtain the one solution shown in the figure above and will not be discussed in the following comparisons of solutions obtained with the three other models: Thomas, Baldwin-Lomax/Thomas, and $k-\epsilon$.

VELOCITY PROFILES FOR FINE GRID SOLUTIONS



Velocity profiles in the plume at three axial locations downstream of the end of the plug are shown in the figure for the fine grid (415 points in the axial direction) solutions. The three locations are all measured relative to the nozzle inflow, as shown in the previous figure of the nozzle geometry. The plot for $X = 25$ in. shows that the $k-\epsilon$ solution has the highest maximum velocity of the three solutions. This is still the case at $X = 50$ in. where the plumes have mixed with the ambient air to lower the maximum velocity of each plume. At $X = 75$ in., the $k-\epsilon$ solution shows the lowest maximum velocity, indicating that the $k-\epsilon$ model calculates more turbulent viscosity in the plume to mix the high energy flow of the jet with the ambient air.

TOTAL TEMPERATURE PROFILES FOR FINE GRID SOLUTIONS



A comparison of total temperature profiles at the same locations as in the previous figure demonstrates the same trend among the turbulence models. At the location nearest the plug tip ($X = 25$ in.), the $k-\epsilon$ solution shows the highest maximum total temperature while downstream at $X = 75$ in., the $k-\epsilon$ solution shows the lowest maximum total temperature. Although the two algebraic turbulence model solutions used different turbulence models in the wall bounded regions near the nozzle, they both used the Thomas model in the region of the flowfield where the jet plume mixes with the ambient air and both demonstrated less mixing in this region than the $k-\epsilon$ solution does. The comparison of Pratt & Whitney nozzle flow calculations that was previously discussed also showed that the NASTAR $k-\epsilon$ solution produced more mixing than the PARC Thomas model solution (although those solutions were obtained not only with different turbulence models but with different codes).

SHOCK FUNCTION (BASED ON PRESSURE GRADIENT)



Thomas



Baldwin-Lomax
/Thomas



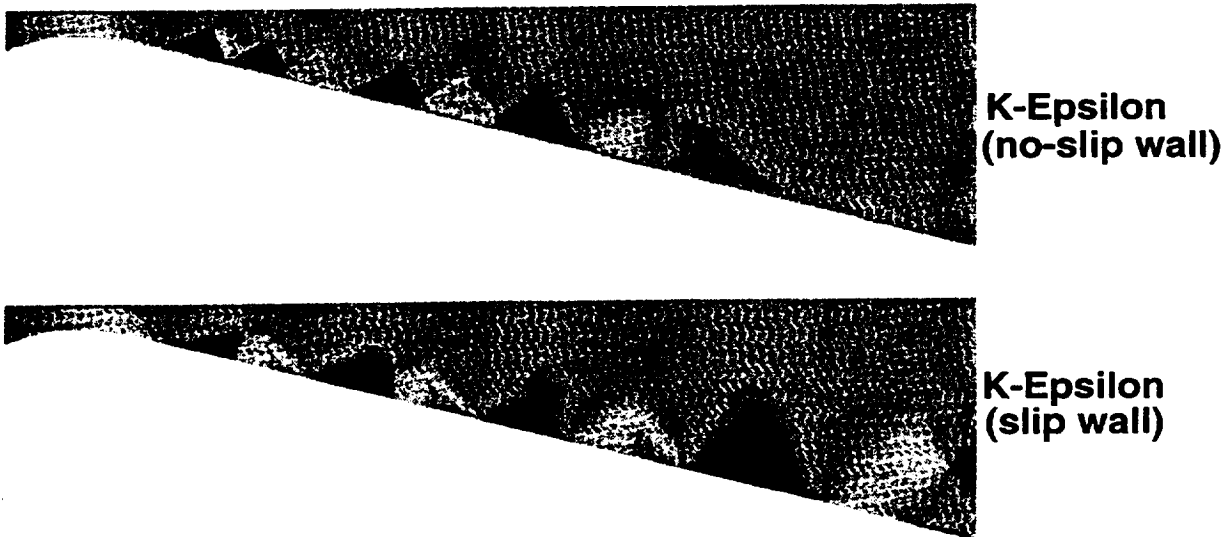
K-Epsilon

The shock function contours in the figure show shock cell patterns that form between the plug and the shear layer (of the jet and ambient air) downstream of the nozzle exit. PLOT3D (used to generate the contour plots) defines this shock function as follows

$$\text{Shock function} = \frac{V}{c} \cdot \frac{\text{grad}(P)}{|\text{grad}(P)|}$$

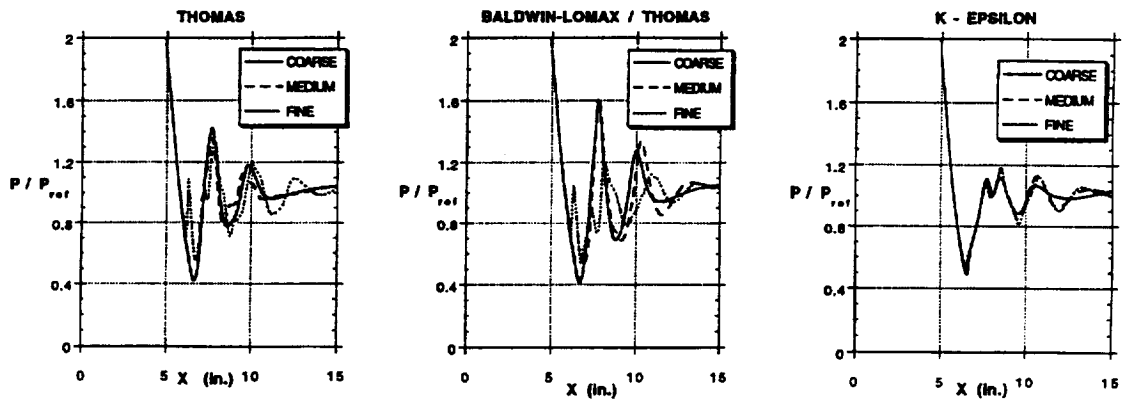
The two solutions obtained with the Thomas and Baldwin-Lomax/Thomas models show that these algebraic models have considerable difficulty in producing realistic looking shock cell patterns. The k- ϵ solution shows a more well defined shock cell pattern. A comparison of these solutions indicates that simple algebraic turbulence models may not be adequate for predicting flow details such as shock cell structure.

EFFECT OF PLUG SURFACE BOUNDARY CONDITION ON SHOCK CELL PATTERN



The figure shows a comparison of shock cell patterns obtained with $k-\epsilon$ using two different boundary conditions for the plug surface. The first was the standard no-slip surface which allows a boundary layer to develop while the second was a slip wall boundary which does not produce a boundary layer. With the standard no-slip boundary, the turbulent viscosity generated in the boundary layer tends to smear the shock structure just outside of the nozzle exit plane. The slip surface boundary case was examined to determine the shock structure without this boundary layer influence. The comparison of the two shock cell patterns demonstrates that the plug surface boundary condition does have a substantial influence on the flow's shock structure, particularly just downstream of the nozzle exit.

STATIC PRESSURE DISTRIBUTION ALONG PLUG



The three plots in the figure show static pressure distributions along the plug for the three turbulence models that were used to obtain solutions with the coarse, medium, and fine grids. The $k-\epsilon$ solutions show much less grid resolution effects on pressure predictions relative to the Thomas and Baldwin-Lomax/Thomas solutions. Both sets of algebraic turbulence model solutions show significant differences in pressure distributions from one grid size to another.

CONCLUDING REMARKS

- **PARC 2D/3D CODES ARE BEING USED TO ANALYZE COMPLEX HSR NOZZLE FLOWS**
- **COMPARISONS TO EXPERIMENTAL DATA SHOW CAPABILITIES/LIMITATIONS OF PARC**
- **FUTURE COMPARISONS WILL DEMONSTRATE EFFECT OF CODE IMPROVEMENTS (TURBULENCE MODELS, ETC.)**

The PARC analyses that have been discussed are only two of the current and planned PARC FNS analyses of HSR nozzles. The comparison of the PARC calculations to experimental data for the Pratt and Whitney 2D mixer-ejector nozzle indicate that PARC is able to predict quantities such as pumping ratio and pressure distributions along the shroud well, while failing to predict the extent of mixing between the primary and secondary flows. The large discrepancy between the PARC solution and the experimental data may be the result of the algebraic turbulence model that was used. If this same flow case is reinvestigated with PARC using the new Speziale $k-\epsilon$ turbulence model, the mixing behavior might change substantially. The Langley single flow plug nozzle tests will provide an excellent set of flow data to compare to the PARC calculations that have already been obtained and those to be obtained in the future.

Several improvements to the PARC code, including addition of new turbulence models and better artificial dissipation schemes, have been implemented or are planned for the future. These improvements will hopefully allow PARC to provide more accurate quantitative flow predictions for HSR-type nozzle flows.

